Proceedings of the ASME 2010 3rd Joint US-European Fluids Engineering Summer Meeting and 8th International Conference on Nanochannels, Microchannels, and Minichannels
FEDSM-ICNMM2010
August 1-5, 2010, Montreal, Canada

FEDSM-ICNMM2010-30333

NUMERICAL SIMULATION OF INTERNAL CAVITIES ACOUSTIC TRAPPED MODES WITH MEAN FLOW

Kareem Aly

McMaster University, Hamilton, ON, L8S 4L7, Canada

Samir Ziada

McMaster University, Hamilton, ON, L8S 4L7, Canada

ABSTRACT

Flow-excited acoustic resonance of trapped modes in ducts has been reported in different engineering applications. The excitation mechanism of these modes results from the interaction between the hydrodynamic flow field and the acoustic particle velocity, and is therefore dependent on the mode shape of the resonant acoustic field, including the amplitude and phase distributions of the acoustic particle velocity. For a cavity-duct system, the aerodynamic excitation of the trapped modes can generate strong pressure pulsations at moderate Mach numbers (M>0.1). This paper investigates numerically the effect of mean flow on the characteristics of the acoustic trapped modes for a cavity-duct system. Numerical simulations are performed for a two-dimensional planar configuration and different flow Mach numbers up to 0.3. A two-step numerical scheme is adopted in the investigation. A linearized acoustic perturbation equation is used to predict the acoustic field. The results show that as the Mach number is increased, the acoustic pressure distribution develops an axial phase gradient, but the shape of the amplitude distribution remains the same. Moreover, the amplitude and phase distributions of the acoustic particle velocity are found to change significantly near the cavity shear layer with the increase of the mean flow Mach number. These results demonstrate the importance of considering the effects of the mean flow on the flow-sound interaction mechanism.

INTRODUCTION

Noise and vibration problems caused by free shear flow over cavities have been reported in the literature for more than 50 years [1]. Rockwell & Naudascher [2] provide an extensive review of cavity flow oscillations. The oscillation of the cavity free shear layer produces acoustic energy that can excite the acoustic resonance inside the cavity itself or of the enclosed domain that the cavity is attached to. The excitation process is self-sustained by a feedback mechanism. The two main components of this mechanism are the inherent instability of the cavity shear layer and the interaction between the free shear layer and the acoustic field. The shear layer instability causes small vorticity perturbations at the cavity leading edge to grow rapidly as they travel downstream with the flow. The amplified vorticity fluctuations interact with the acoustic particle velocity (the velocity fluctuation associated with the resonant acoustic field) near the cavity downstream edge such that part of the flow perturbation energy is transformed into acoustic energy to excite, or sustain the excitation of the acoustic resonance. Subsequently, the particle velocity of the excited acoustic mode triggers the free shear layer near the cavity upstream edge to close the feed-back loop, and thereby starts a new cycle of oscillation. From this cycle of events, it is clear that the excitation process is strongly dependent on the shape of the resonant acoustic mode, and therefore the effect of the mean flow on the amplitude and phase distributions of the resonant acoustic mode needs to be clarified.

Flow over cavities is known to be capable of exciting different types of acoustic resonances. For example, the acoustic modes of the cavity volume "alone" can be excited for deep cavities at low Mach number flows (East [3], Ziada [4]) shallow cavities can also be excited by grazing flows, but only at moderate and high Mach numbers [5; 6]. At low Mach numbers, unconfined shallow cavities do not generally produce strong resonances because of the associated high radiation damping. However, when they are confined, the acoustic modes of the confinement can be strongly excited by low Mach number flows over shallow cavities. For example, Davies [7], Nomoto and Culick [8], Rockwell & Schachenmann [9; 10], Stubos et al. [11] and Geveci et al. [12] investigated the coupling between an internal cylindrical cavity and the longitudinal acoustic modes in the attached pipes. The longitudinal modes here refer to the acoustic plane waves along the main flow duct. On the other hand, the acoustic trapped modes of ducted cavities can strongly be excited by the oscillation of the cavity shear layer. Keller &

Escudier [13] and Ziada et al. [14] studied experimentally the coupling between the cavity shear layer and the trapped modes of the cavity-duct system. The excitation of trapped modes can generate excessively high sound pressure levels as a result of their low radiation losses.

Many researchers studied the momentum and energy exchanges occurring between the hydrodynamic field and the acoustic field e.g. [15; 16; 17], by the superposition the acoustic field and the fluctuating hydrodynamic field. It has been shown that the relative phase between the vorticity field and the acoustic particle velocity of the resonant mode is the controlling parameter for whether the acoustic energy will be produced or absorbed by the vorticity field. Also, the amount of energy generation (or absorption) depends on the amplitude of the acoustic particle velocity where the energy exchange takes place [18]. However, to the author knowledge, all the studies reported in the literature, consider the acoustic field at zero flow velocity; and thereby ignore the effects of the mean flow and the coupling mechanism on the amplitude and phase distributions of the particle velocity associated with the resonant acoustic mode. This approach is based on the argument that these effects are negligibly small as long as the Mach number of the mean flow is small. This argument has not been critically examined to date.

To examine the effect of the mean flow on the acoustic particle velocity, a numerical model is developed to simulate this phenomenon. The work presented in this paper predicts the effect of mean flow on the trapped mode shape of a ducted cavity. The excitation of this type of modes has been reported for various valve configurations including, for example, gate valves [19]. Keller & Escudier [13] studied the excitation of these modes at Mach numbers close to unity and Ziada et al. [14] found that the excitation level is proportional to the Mach number. The latter authors reported also that self-sustained resonances can occur at Mach numbers as low as 0.1. More recently, Aly and Ziada [20] reported acoustic resonances of the lowest three trapped modes of a cavity-duct system at Mach numbers ranging from 0.1 to 0.4 Therefore, determining the effect of the mean flow on the acoustic field will allow for better understanding of the excitation mechanism and for the development of suitable suppression techniques.

Acoustic trapped modes are known to exist in unbounded fluids and wave guides where the perturbation energy is localized in regions accommodating some changes in the domain geometry or the fluid properties [21]. For the cavity-duct configuration, the cavity represents the geometrical change which introduces the trapped mode to the system response. The acoustic pressure of the trapped mode along the wave guide decays exponentially with the distance from the cavity. Duan et al. [22] determined numerically the characteristics of the trapped modes at zero flow velocity for a two-dimensional cavity-duct system. These modes have a vanishingly small imaginary part which corresponds to small radiation from the ducts ends. Hein and Koch [23] and Koch [24] extended Duan et al's work and predicted numerically the existence of "nearly trapped" diametral modes for axisymmetric cavity-duct configurations, also for zero flow condition. In practice, these modes can be strongly excited by the flow over the cavity opening [20], as they experience very small damping.

The effect of the mean flow on the resonance frequency of flat plate cascade was studied by Koch [25]. Lee [26] studied the effect of the mean flow Mach number on the resonance mode of a wind-tunnel with plenum. Both, Koch and Lee reported decrease in the resonance frequency with the increase of the Mach number. Moreover, Lee reported that the mode shape at the slotted wall between the wind-tunnel and the plenum changes with the increase of the Mach number. Also, the effect of the mean flow on the acoustic resonance of constant and variable area ducts has received considerable attention by researchers working in the area of sound propagation and radiation from jet engine fans. For example, Eversman [27], Nayfeh et al. [28] and Li et al. [29] are among numerous authors who studied the effect of mean flow on the sound propagation in ducts. Eversman [30] provides a comprehensive review of this subject.

In this paper, the results of a numerical simulation of trapped modes are presented for the case of a cavity-duct system with mean flow. The objective is to explore the effect of the mean flow on various aspects of the resonance mode characteristics, such as the amplitude and phase distributions of the acoustic pressure and particle velocity. In order to validate the accuracy of the simulation, the trapped mode frequency obtained from the simulation will be compared with the experimental data. The numerical approach and schemes are outlined in section 2. The technique of determining the frequency of the trapped mode is described in section 3. In section 4, the characteristics of the first (or lowest) trapped mode of the 2-D planar cavity-duct system are presented.

NUMERICAL APPROACH

A two-step approach was adopted to allow consideration of the effect of the mean flow on the acoustic mode shape and frequency. In the first step, the mean flow was simulated by solving steady state Reynolds Average Navier-Stokes equations. A commercial finite volume code was used. The turbulence quantities were modeled using Reynolds stress model to ensure accurate treatment of the free shear layer. The unsteady acoustic field is simulated in the second step, which involves solving a system of linearized acoustic perturbation equations. This approach allows the investigation of the effect of the mean vorticity and velocity gradient, in addition to the convection effect, on the acoustic field. However, the effect of the energy exchange on the mode shape is not considered because at the trapped mode frequency, the radiation damping is very small and the amount of energy exchange at the shear layer becomes relatively small compared to the total acoustic energy in the computation domain.

A FORTRAN finite difference code was developed to solve the lineariezed acoustic perturbation equations. The system of governing equations and the schemes used to calculate the spatial and temporal derivatives are discussed in the next subsections.

System of governing equations

A linearized system of "Acoustic Perturbation equations" (APE), developed by Ewert & Schröder [31], was used to describe the acoustic propagation. Unlike the linearized Euler equations (LEE), the APE does not support the vorticity equation. Therefore, APE can be used to simulate the acoustic field in the free shear layer region without suffering from the excitation of the hydrodynamic instability. Ewert & Schröder [31] separated the different eigienmodes of the linearized Euler equations in the frequency wave number domain. The eigenmodes governing the vorticity and entropy wave were then removed and the system of equations was transferred back to the spatial-time domain. The resulting APE for multidimensional domain without source terms can be written as follows:

$$\frac{\partial p_a}{\partial t} + c^2 \nabla \left(\rho_0 \vec{U}_a + \vec{U} \frac{p_a}{c^2} \right) = 0 \qquad 1$$

$$\frac{\partial U_a}{\partial t} + \nabla\left(\vec{U}.\vec{\mathrm{U}}_{\mathrm{a}}\right) + \nabla\left(\frac{p_a}{\rho_0}\right) = 0 \qquad 2$$

where, p_a is the acoustic pressure perturbation, $\vec{U}_a$ is the acoustic particle velocity vector, $\vec{U}$ is the mean velocity obtained from the simulation of the RANS equations, ρ_0 is the mean density and c is the mean acoustic speed, which is set to 340 m/s. The source terms are ignored as they describe mainly the effect of the turbulence or the entropy fluctuations on the acoustic field.

Calculation of the spatial derivatives

The spatial derivatives were calculated using the three points stencil optimized prefactored compact finite difference scheme developed by Ashcroft & Zhang [32]. This scheme is a fourth order accurate with low dissipation and low dispersion characteristics. Therefore, this scheme is suitable for accurate simulation of acoustic wave propagation. Also, this scheme requires a relatively small stencil, as well as fewer boundary stencils that allow a simple formulation of the boundary conditions. A minimum of 5 points per wavelength is needed to accurately resolve the propagation of a certain wave.

Time marching scheme

A two-step 5/6 stages low-dissipation and low dispersion Runge-Kutta scheme (LDDRK) was used to perform the numerical integration with time [33]. This is a fourth order accurate scheme with optimized coefficients to minimize the numerical dissipation and dispersion. This optimization increases the time step limit that is based on the level of numerical dissipation. The 2N-storage form of the scheme [34] is used. An 8th – order filter is also applied at each stage of the Runge-Kutta scheme [35].

Treatment of the boundary conditions

Appropriate numerical boundary conditions are needed to be implemented for each boundary of the computational domain including hard wall and duct open ends. The description of each numerical boundary condition is given in the following.

Wall boundary condition At the grid nodes of the wall, the velocity is set to zero and the velocity derivative in the perpendicular direction on the wall is calculated using one-sided explicit formulas provided by Ashcroft & Zhang. [32].

Zero pressure boundary condition The pressure is set to zero at the inlet and outlet of the cavity-duct system. This boundary condition reflects all pressure waves back inside the domain. The rationale behind this implementation is discussed later on with the presentation of the simulation results. It suffices to mention here that the simulated cross-mode has been found to be either trapped or nearly trapped [23] which has a negligibly small radiation damping. The pressure derivative perpendicular to the boundary is calculated using the same one sided explicit formulas [32]. The velocity derivative perpendicular to the boundary is set to zero.

DETERMINATION OF THE RESONANCE FREQUENCY

The first step to simulate the acoustic resonance is to determine the frequency of the resonance mode of interest. Experimentally, the resonance frequency can be determined by exciting the physical domain using a loudspeaker driven by a random signal. Using a technique analogous to this experimental method, the numerical domain is excited by a broadband excitation by vibrating the cavity floor.

To produce a broadband excitation, the cavity floor was forced to oscillate according to the following function:

$$v_e(t) = 0.5 \frac{\sin(2\pi f_e(t - \mathrm{aa}))}{2\pi f_e(t - \mathrm{aa})} \qquad 3$$

where $v_e(t)$ is the instantaneous vertical velocity of the cavity floor, f_e is the maximum frequency of excitation, aa is a shift in the time to ensure that the vibration at the beginning of the simulation has low amplitude, as shown in Fig. 1. This prevents the generation of high frequencies in the solution due to the discontinuity of the initial condition, which cannot be handled by the numerical grid.

The Fourier analysis of the cavity floor oscillation function shows that the cavity floor oscillation can be described by a rectangular function in the frequency domain= $\frac{1}{f_e} rect\left(\frac{f}{2f_e}\right)$. The rectangular function is described as follow:

$$rect\left(\frac{f}{2f_e}\right) = \begin{cases} 0 & \left|\frac{f}{2f_e}\right| > \frac{1}{2} \\ \frac{1}{2} & \left|\frac{f}{2f_e}\right| = \frac{1}{2} \\ 1 & \left|\frac{f}{2f_e}\right| < \frac{1}{2} \end{cases} \qquad 4$$

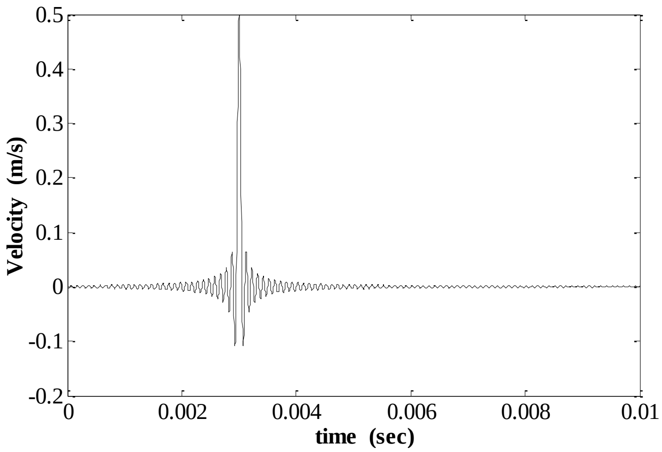

Figure 1 Time signal of the cavity floor forced oscillation

Figure 2 shows the amplitude spectrum of the cavity floor vibration velocity as implemented in the program. The amplitude and the shape of the perturbation agree perfectly with the analytical formula given by equation 4.

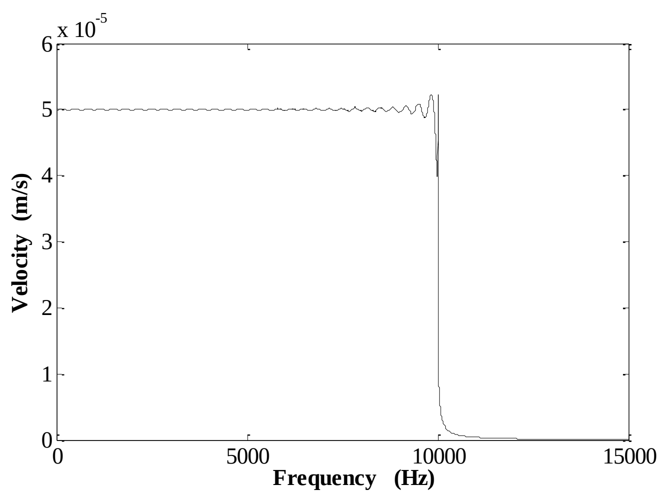

Figure 2 Amplitude spectra of the cavity floor forced oscillation

Figure 3 shows the amplitude spectrum of the pressure fluctuation corresponding to the 2-D cavity duct system excited by the forced oscillation described by equation 3. The 2-D duct has 2 cavities attached to the middle of the duct on the top and bottom walls. The cavities are 25 mm in length and 25 mm in depth and the duct height is 150 mm. The amplitude spectrum is for pressure time trace at the middle of the cavity floor. The maximum frequency, f_e, of the random excitation was set to 10000 Hz. The floors of both cavities were forced to oscillate out-of-phase to excite the first trapped cross-mode and to avoid exciting the longitudinal modes. The power spectrum shows a strong peak at 1109 Hz which corresponds to the first trapped mode. The finite element analysis solving the mass-stiffness matrix for the same geometry without flow results in a frequency of 1112 Hz. This demonstrates the good agreement between the current methodology, in the case of zero flow velocity, and the solution of the mass-stiffness matrix. As can be seen in Fig. 3, numerous other peaks with smaller amplitudes appear in the spectrum. These peaks represent the combined cross-longitudinal modes.

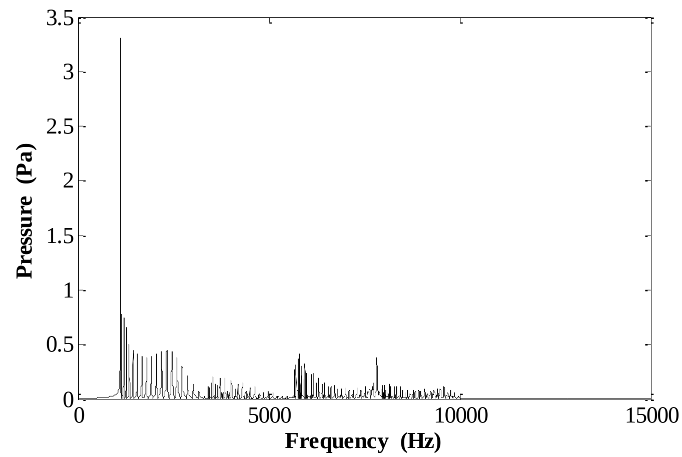

Figure 3 Spectrum of the pressure fluctuation resulting from the broad band excitation of the numerical domain

RESULTS OF THE 2-D PLANAR GEOMETRY

The results of this section detail the changes which occur in the first trapped mode with the increase in the mean flow velocity. First, the results of random excitation at different flow Mach numbers are presented to show the effect of the mean flow field on the acoustic mode frequency. This is followed by the simulation results showing the effect of the mean flow field on the acoustic mode shape.

The trend of the frequency change obtained from the simulation is compared with the experimental data reported by Aly [36]. To simplify the comparison, the dimensions of the simulation domain are chosen to be the same as those of the test rig used by Aly [36]. Figure 4 shows a schematic of the geometry of the 2-D cavity-duct system. The duct has 2 cavities attached at its center to the top and bottom walls. The cavities are 25 mm long and 25 mm deep. The duct height is chosen to be 150 mm. A relatively long duct, 2 m, is considered to ensure that the artificial boundary conditions of zero pressure at the duct ends would not influence the general behaviour. Three different mean flow Mach numbers (0.1, 0.2, and 0.3) were simulated in addition to the case of zero flow.

Effect of mean flow on the resonance frequency

The cavity-duct geometry was simulated considering different average mean flow Mach number. A uniform mesh with grid spacing of 1.5625 mm was used in the simulation of the different flow rates. With this grid spacing, about eight grid points existed within the free shear layer thickness. This is to ensure adequate representation of the effect of the velocity gradient of the free shear layer on the pressure wave propagation and to minimize the generation of spurious wave due to corner singularity. Reducing the grid spacing to 1.25 mm changed the resonance frequency by about 0.5% at low Mach number. Therefore, the 1.5625 mm grid spacing was used in the simulation of all the cases to ensure no effect from changing the grid spacing on the comparison between the resonance frequencies of the different flow Mach number cases.

Figure 5 shows the resonance frequency of the first trapped mode (f_1) for different mean flow Mach numbers as a ratio to the resonance frequency at zero flow (f_1(M=0)). At zero flow velocity, the trapped mode frequency is 1109 Hz, which is about 0.98 of the cut-off frequency of the main duct. Referring to Fig. 5, the numerical results show that the resonance frequency decreases with the flow Mach number. The rate of the frequency drop increases with the Mach number. Similar behaviour was observed in the experimental results of Aly [36] as shown in Fig. 5, and in the numerical simulation results reported by Koch [25] and Lee [26] for other flow configurations. The experimental data shown in Fig. 5 corresponds to a cavity with 12.5 mm depth and 50 mm length. This experimental case has a trapped mode frequency at a very low flow velocity of about 0.975 of the main duct cut-off frequency. This ratio proved to be a good dimensionless parameter that can be used to characterize the impact of the mean flow on the resonance frequency. At a Mach number of 0.3, the difference between the experimental and numerical dimensionless frequencies is about 0.008 which is considered good given all the simplifications implemented in the numerical model.

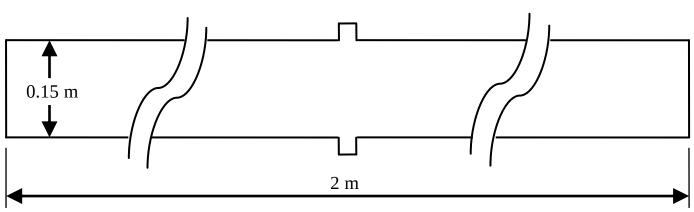

Figure 4 Schematic of the 2-D computational domain. Cavity length is 25 mm and cavity depth is 25 mm

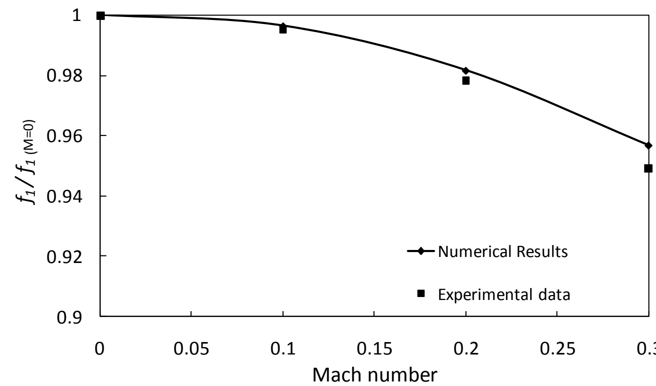

Figure 5 Dimensionless frequency of the trapped mode as a function of the mean flow Mach number

Effect of mean flow on the mode shape

In this section, the effect of the mean flow on the mode shape of the first trapped acoustic mode is discussed. This includes the characterization of the mean flow effect on the spatial distributions of: (a) the acoustic pressure; (b) the acoustic pressure phase; (c) the particle velocity amplitude and (d) the particle velocity phase.

To obtain the pressure and particle velocity fields, the numerical domain, which is shown in Fig. 4, is excited at the resonance frequency by vibrating the cavity floor. This artificial method of exciting the domain has no effect on the mode shape because trapped acoustic mode under consideration is very lightly damped. Consequently, the ratio of the input energy to the acoustic energy inside the domain at steady state is small. Therefore, this excitation method does not change the shape of energy distribution in the domain. The grid spacing used is the same as described in the previous section for the random excitation to ensure the same resonance frequency in both cases. The solution for the pressure field amplitude and phase was considered adequate when the cycle-to-cycle change of the maximum pressure amplitude at the cavity floor became less than 0.5% of the maximum amplitude. This requirement ensured that the effect of transient response on the results is negligible.

Amplitude of the acoustic pressure Figure 6 shows the contour plot of the pressure amplitude of the first trapped acoustic mode of the planar cavity-duct system. The plot corresponds to zero mean flow velocity. The plot shows that the maximum pressure amplitude is located at the center of cavity floor. The amplitude decreases with the distance from the cavity center. This agrees with the general description of the cross-modes of symmetric ducts. For the cases with mean flow Mach numbers of 0.1, 0.2 and 0.3, the distributions of the pressure amplitude are found to be generally similar to those shown in Fig. 6.

Figure 7 shows the ratio of the pressure amplitude along the duct wall and the cavity mouth to the pressure amplitude at

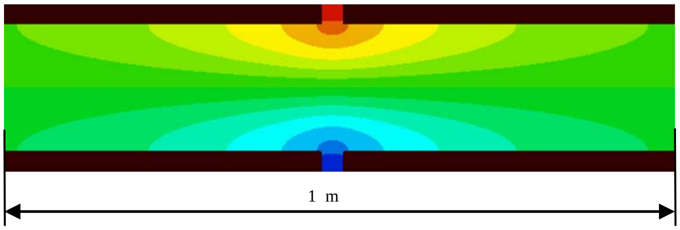

Figure 6 Contours of the pressure amplitude of the first transverse acoustic mode of planar cavity-duct system. M=0, L=25mm, d=25mm and the duct height = 150mm.

the middle of the cavity floor for the four simulated mean flow Mach numbers. In all simulations presented in this paper, the flow direction is from the left to the right and the x-axis is the distance measured from the center of the cavity. The pressure amplitude is seen to decay exponentially with distance from the cavity in all four cases. According to Kinsler et al. [37], the exponential decay of a transverse wave with a frequency below the cut-off frequency of a constant cross-section infinite wave guide is given as follows:

$$P_a(x) = Ae^{-kk\,x} \qquad 5$$

$$kk = \frac{\sqrt[2]{\omega_k{}^2-\omega^2}}{c} \qquad 6$$

where, $P_a(x)$ is the pressure amplitude in the x-direction, ω_k is the cut-off frequency of the wave guide (rad/s), ω is the frequency of the decaying transverse wave (rad/s) and c is the speed of sound.

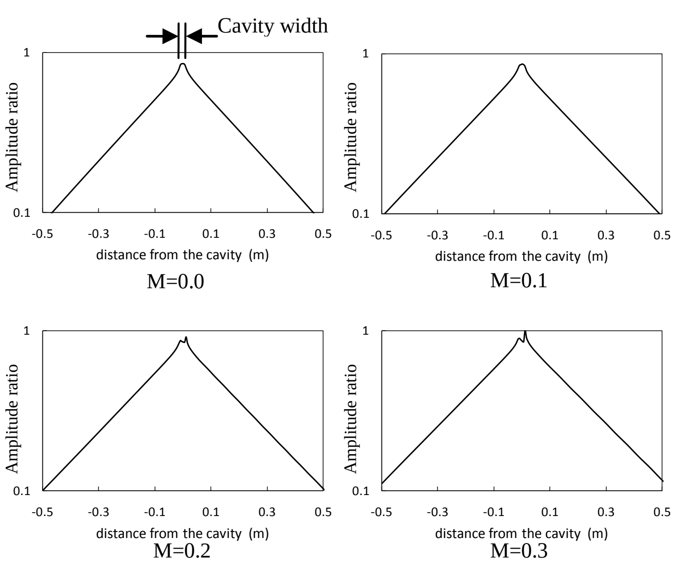

Figure 7 Simulation results of the planar cavity-duct system showing the acoustic pressure amplitude along the duct wall as a ratio to the amplitude of the pressure at the centre of the cavity floor. Flow direction is from right to lift

For the case of zero flow, the cut-off frequency of the main duct is 1133.3 Hz and the trapped mode frequency is 1109 Hz. Using equation 6, the exponential decay coefficient, kk, for the case of zero flow velocity is 4.32 m^{-1}. From the numerical results, the exponential decay exponent is 4.47 m^{-1}. This indicates acceptable level of accuracy in predicting the acoustic wave propagation using the current numerical method. For the other flow velocities, the exponential decay coefficient decreases with the increase of the flow Mach number. At a Mach number of 0.3, the decay coefficient is 4.15 m^{-1} upstream of the cavity and 4.0 m^{-1} downstream of the cavity. The difference in the rate of decay between the upstream and downstream sides of the duct is evident in all simulated cases. However, in all the cases, the pressure amplitude 0.5 m away from the center of the cavity is an order of magnitude lower than the amplitude at the cavity center. If the same exponential decay is maintained for the rest of the simulated duct, the pressure amplitude at the duct termination, 1 m away from the cavity, will be two-order of magnitude lower than at the center of the cavity. Therefore, the artificial reflective boundary condition which is applied at the duct ends has extremely small effect on the mode shape. This is also evident in the perfect exponential decay predicted by the simulation.

Referring again to Fig. 7, the pressure amplitude at the cavity mouth is around 84% of the pressure amplitude at the cavity floor in the case of zero flow. As the Mach number increases, the pressure amplitude increases near the downstream edge of the cavity. At a Mach number of 0.3, the pressure amplitude at the downstream edge is almost equal to the amplitude at the center of the cavity floor.

Phase of the acoustic pressure It is well known that, at zero flow, the change in the phase of the acoustic pressure of the trapped acoustic mode along the axial direction of the duct is zero. In the transverse direction, the phase change is zero everywhere except across the duct centerline, where the pressure switches polarity and a phase jump of 180^0 occurs. The current numerical results follow exactly this description at zero flow velocity. However, the numerical results show an axial change in the pressure phase when the mean flow velocity is greater than zero. Figure 8 shows several snap shots of the pressure contours over almost half a cycle. Note that the snap shots are equally spaced in time, the mean Mach number is 0.2 and the flow direction is from the left to the right. As shown in these contour plots, the pressure mode shape travels upstream in the opposite direction to the flow. The traveling speed (group speed) and consequently the axial phase distribution are found to depend on the Mach number.

Figure 9 shows the distribution of the phase of the acoustic pressure in the axial direction for Mach numbers of 0.1, 0.2 and 0.3. These results correspond to the trapped mode pressure distributions shown in Fig. 7. The phase of the pressure at the mid-length of the top cavity floor is taken as a reference during the phase calculation. To determine the phase at a selected point, the time period between the occurrence of maximum pressure amplitude at this point and the occurrence of maximum amplitude at the middle of the cavity is calculated. Thereafter, this time difference is multiplied by the angular frequency to determine the phase difference between the selected point and the middle of the cavity floor. This procedure is repeated for all the grid point to obtain a comprehensive picture of the phase change within the computational domain.

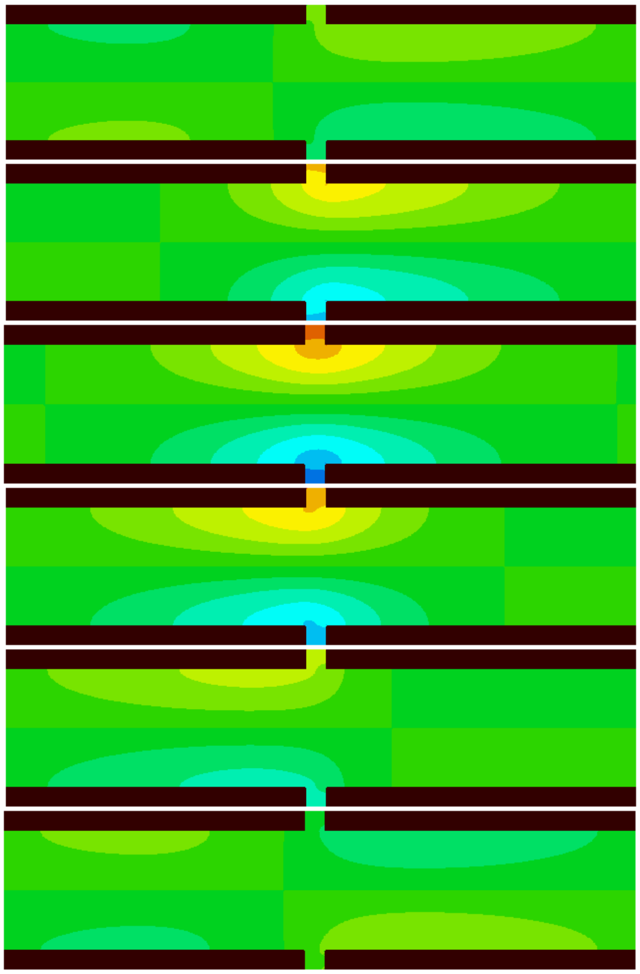

Figure 8 Snap shots of the contours of the acoustic pressure over half a cycle of the trapped mode of the cavity-duct system. The contours amplitude is linearly distributed from +1 to -1. M=0.2.

As can be seen in Fig. 9, the rate of the axial phase change of the trapped mode appears to be constant along the axial direction. This rate increases with the increase of the Mach number. It is noteworthy that there is no phase change in the transverse direction except the change of pressure polarity at the center line, see Fig. 8. To quantify the rate of the phase change, the axial phase speed was calculated. The phase speed is the speed at which the phase is propagating in a certain direction. The local phase speed was calculated as follow:

$$c_p = -\omega \frac{\Delta x}{\Delta \text{phase}} \qquad 7$$

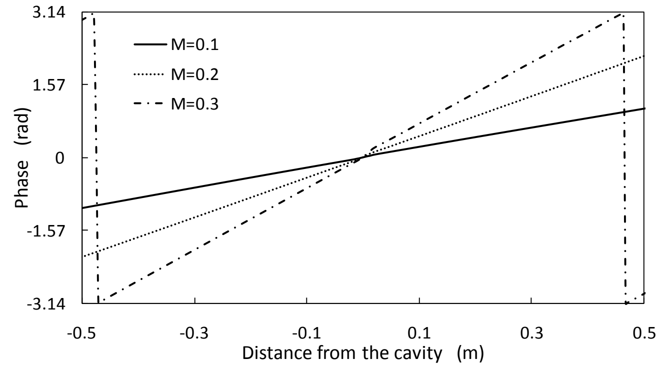

Figure 9 Simulation results of the first trapped mode of the planar cavity-duct system showing variation of the pressure phase in the axial direction along the duct wall.

where, $\boldsymbol{\omega}$, is the angular frequency. The negative sign indicates that when $\frac{\Delta x}{\Delta \text{phase}}$ is positive the wave propagates in the negative $\mathbf{x}$-direction. Figure 10 shows the distribution of the absolute value of the phase speed along the axial direction for M=0.2. The average phase speed away from the middle of the duct, where the cavity is located, is about 1595 m/s. In the vicinity of the cavity location, the phase speed decreases. This phenomenon is observed also in the results of M=0.1 and 0.3. The average phase speed for M=0.1 and 0.3 is about 3290 m/s and 1010 m/s, respectively. Similar behaviour was predicted for transverse modes of straight ducts [30].

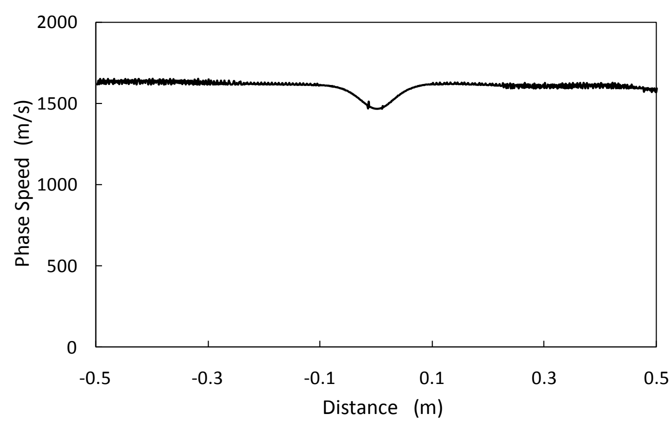

Figure 10 Simulation results of the first trapped mode of the planar cavity-duct system showing axial Phase speed of the pressure for M=0.2.

Amplitude of the acoustic particle velocity The acoustic power production during the aerodynamic excitation of the acoustic resonance depends on amplitude and phase distributions of the acoustic particle velocity of the resonant mode. More specifically, for the two-dimensional geometry under investigation, Fig. 4, the power production is strongly

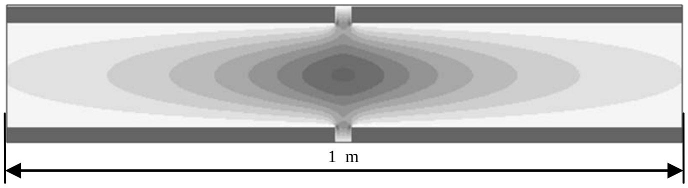

Figure 11 Simulation results of the planar cavity-duct system showing the contour plot of the amplitude of the vertical particle velocity at zero flow for the first trapped mode.

related to the vertical component of the acoustic particle velocity. Therefore, this section focuses on the characteristics of the particle velocity vertical componernt. Figure 11 shows the contour plot of the vertical particle velocity for zero flow condition. The results for Mach numbers of 0.1, 0.2 and 0.3 are found to be similar to the zero flow condition near the centerline of the duct, except that the location of the maximum particle velocity at the centerline shifts slightly downstream as the Mach number increases. As an example, for Mach number of 0.3, the location of the maximum particle velocity shifts by 7 mm downstream. However, the main changes in the amplitude of the vertical particle velocity occur at the cavity mouth where the acoustic power is produced.

Figure 12 shows the contour plots of the vertical particle velocity near the cavity mouth for the four studied flow Mach numbers. All figures correspond to the same acoustic pressure at the center of the cavity floor. At zero flow, the distribution of the particle velocity amplitude is symmetric with the amplitude increasing near the cavity edges. For a Mach number of 0.1, the amplitude is higher near the upstream edge of the cavity. For Mach numbers of 0.2 and 0.3, the maximum amplitude starts to move toward the downstream edge. These results underline the significant change in the distribution of the vertical particle velocity with the mean flow Mach number, and its consequent effect on the mechanism of sound generation during acoustic resonance.

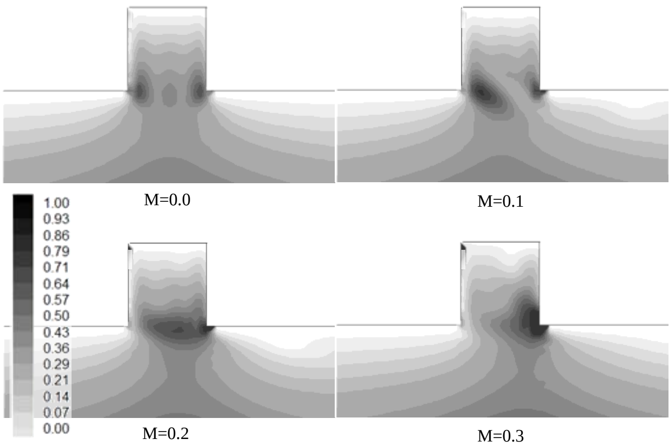

Figure 12 Contour plots of the amplitude of the vertical particle velocity for the first trapped mode of the planar cavity-duct system. The contours legend is just to demonstrate the relative amplitude of the contours.

Phase of the acoustic particle velocity The phase distribution of the acoustic particle velocity is important in determining the Strouhal number at which the aerodynamic excitation of the trapped mode reaches its maximum strength. In this section, the change in the phase distribution of the vertical particle velocity with the mean flow Mach number is discussed. Figure 13 shows four snap shots of the vertical particle velocity contours over half a cycle. The snap shots are equally spaced in time. The Mach number for these snap shots is 0.2 and the flow direction is from the left to the right side. As shown in the contour plots, the vertical particle velocity distribution follows the pressure in the main duct, Fig. 8, by traveling upstream in the opposite direction to the flow. However, in the area surrounding the cavity free shear layer and inside the cavity, the contours of the vertical particle velocity progress downstream with the mean flow. Similar behaviour is observed in the other two cases with M=0.1 & 0.3.

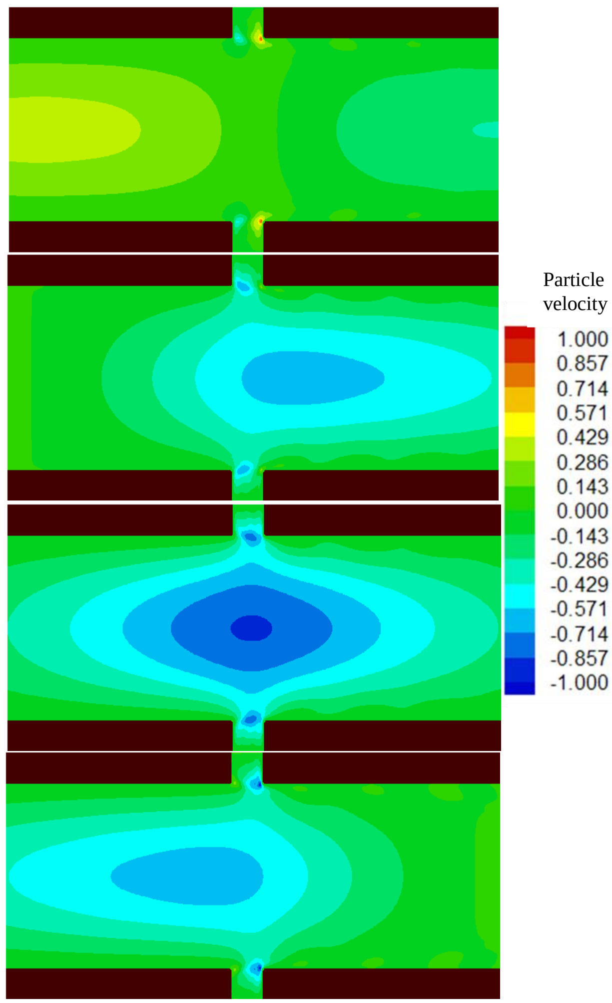

Figure 13 Simulation results of the first trapped mode of the planar Cavity-duct system showing snap shots of the vertical particle velocity contours for M=0.2. The contours legend is just to demonstrate the relative amplitude of the contours

Figure 14 shows the distribution of the phase of the vertical particle velocity along the cavity mouth of the top cavity for Mach numbers of 0.1, 0.2 and 0.3. The axial distance is normalized by the cavity length *L*. The phase of the acoustic pressure at the mid-length of the top cavity floor is taken as a reference during the phase calculation. The phase is calculated following the same procedure used to calculate the phase distribution of the pressure. For zero flow, the numerical results show that the phase between the pressure and particle velocity is nearly constant with an average of $\pi/2$, which agrees with the analytical results of constant phase of $\pi/2$. The small error in the numerical solution arises from the physical singularity at the cavity corners. For Mach numbers of 0.2 and 0.3, the phase distribution over the mouth is almost linear. For Mach number of 0.1, the phase decreases steadily over the upstream half of the cavity mouth and fluctuates around $\boldsymbol{\pi/2}$ over the downstream half. The rate of the phase change decreases slightly with the increase in the Mach number and, on average, the phase difference increases with the increase of the Mach number.

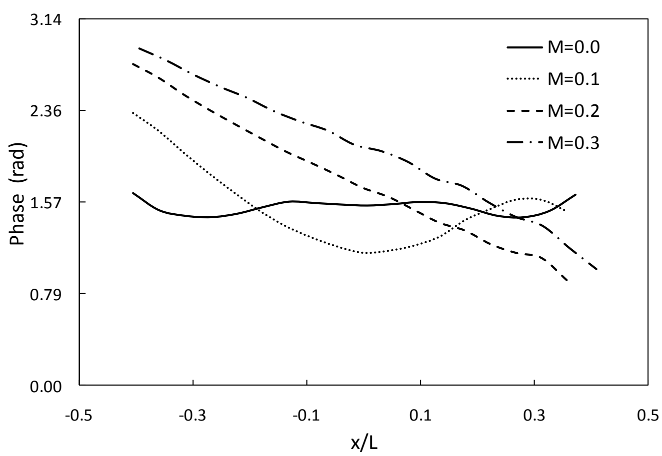

Figure 14 Phase of the vertical particle velocity along the cavity mouth for the first trapped mode of the planar cavity-duct system.

CONCLUSIONS

A numerical code has been developed to study the effect of the mean flow on the trapped mode of 2-D planar cavity-duct systems. Four different mean flow Mach numbers (M= 0.0, 0.1, 0.2 & 0.3) have been considered in the investigation.

The numerical simulation shows that the frequency of the acoustic mode decreases with the increase of the mean flow Mach number. This is in full agreement with the experimental results reported for similar flow geometry As a result of the mean flow convection of the acoustic field an axial phase gradient of the acoustic pressure and particle velocity is developed. The phase speed corresponding to this gradient is in the opposite direction of the mean flow, except near the cavity mouth where the particle velocity phase speed is in the same direction as the mean flow. The amplitude of the pressure field does not change noticeably due to the mean flow. However, the particle velocity amplitude near the cavity mouth changes significantly with the mean flow. These changes in the amplitude and phase of the particle velocity are bound to influence the sound production process when trapped modes are excited by the mean flow, even at relatively low Mach numbers.

REFERENCES

1) J. E. Rossiter, The effect of cavities on the buffeting of aircraft, Royal Aircraft Establishment-Tech. Mem., 754 (1962).

2) D. Rockwell, E. Naudascher, Review: Self-sustaining oscillations of flow past cavities, Journal of Fluids Engineering, 100 (1978) 152-165.

3) L. F. East, Aerodynamically induced resonance in rectangular cavities, Journal of Sound and Vibration, 3 (1966) 277–287.

4) S. Ziada, A Flow visualization study of flow- acoustic coupling at the mouth of a resonant side-branch, Journal of Fluids and Structures, 8 (1994) 391-416.

5) J. E. Rossiter, Wind-Tunnel Experiments on the Flow over Rectangular Cavities at Subsonic and Transonic Speeds, ARC/R&M-3438, 1966.

6) O. H. Unalmis, N. T. Clemens, D. S. Dolling, Cavity oscillation mechanisms in high-speed flows. AIAA Journal, 42 (2004) 2035-2041.

7) P. Davies, Flow-acoustic coupling in ducts, Journal of Sound and Vibration, 77 (1981) 191–209.

8) H. Nomoto, F.E.C. Culick, An experimental investigation of pure tone generation by vortex shedding in a duct, Journal of Sound and Vibration, 84 (1982) 247-252.

9) D. Rockwell, A. Schachenmann, Self-generation of organized waves in an impinging turbulent jet at low Mach numbers, Journal of Fluid Mechanics, 117 (1982) 425–441.

10) D. Rockwell, A. Schachenmann, The organized shear layer due to oscillations of a turbulent jet through an axisymmetric cavity, Journal of Sound and Vibration, 87 (1983) 371–382.

11)A.K. Stubos, C. Benocci, E. Palli, G.K. Stoubos, D. Olivari, Aerodynamically generated acoustic resonance in a pipe with annular flow restrictors, Journal of Fluids and Structures, 13 (1999) 755-778.

12)M. Geveci, P. Oshkai, D. Rockwell, J. C. Lin, M. Pollack, Imaging of the self-excited oscillation of flow past a cavity during generation of a flow tone, Journal of Fluids and Structures, 18 (2003) 665-694.

13)J. J. Keller, M. P. Escudier, Flow-excited resonances in covered cavities, Journal of Sound and Vibration, 86 (1983) 199-226.

14)S. Ziada, H. Ng, C. E. Blake, Flow excited resonance of a confined shallow cavity in low Mach number flow and its control, Journal of Fluids and Structures, 18 (2003) 79-92.

15)P.A. Nelson, N.A. Halliwell, P.E. Doak, Fluid dynamics of a flow excited resonance-Part II: flow acoustic interaction, Journal of Sound and Vibration, 91 (1983) 375–402.

16)J.C. Bruggeman, A. Hirschberg, M.E.H. Dongen, A.P.J. Wijnands, J. Gorter, Flow induced pulsations in gas transport systems: analysis of the influence of closed side branches, Journal of Fluids Engineering, 111 (1989) 484-491.

17)K. Hourigan, M. C.Welsh, M. C. Thompson, A. N. Stokes, Aerodynamic sources of Acoustic Resonance in a duct with Baffles, Journal of Fluid and Structures, 4 (1990) 345-370.

18)M.S. Howe, Contributions to the Theory of Aerodnamic Sound, with Application to Excess Jet Noise and the Theory of the Flute, Journal of Fluid Mechanics, 71 (1975) 625-673.

19) P. Lafon, S. Caillaud, J.P. Devos, C. Lambert, Aeroacoustical coupling in a ducted Shallow cavity and fluid/structure effects on a steam line, Journal of Fluids and Structures, 18 (2003) 695-713.

20) K. Aly, S. Ziada, Flow-excited resonance of trapped modes of ducted shallow cavities. Journal of Fluids and Structures, (2009), doi:10.1016/j.jfluidstructs.2009.07.008.

21) D.V. Evans, M. Levitin, D. Vassiliev, Existence theorems for trapped modes, Journal of Fluid Mechanics, 261 (1994) 21-31.

22) Y. Duan, W. Koch, C.M. Linton, M. McIver, Complex resonance and trapped modes in ducted domains, Journal of Fluid Mechanics, 571 (2007) 119-147.

23) S. Hein, W. Koch, Acoustic resonances and trapped modes in pipes and tunnels, Journal of Fluid Mechanics, 605 (2008) 401-428.

24) W. Koch, Acoustic resonances and trapped modes in annular plate cascades, Journal of fluid mechanics, 628 (2009) 155–180.

25) W. Koch, Resonant acoustic frequencies of flat plate cascade, Journal of Sound and Vibration, 88 (1983) 233-242.

26) I. Lee, Plenum chamber effect on wind-tunnel resonance by the finite-element method, AIAA Journal, 26 (1988) 1087-1093.

27) W. Eversman, Energy flow criteria for acoustic propagation in ducts with flow, Journal of Acoustic Society of America, 49 (1971) 1717-1721.

28) A. Nayfeh, J.E. Kaiser, D.P. Telionis, Acoustics of aircraft engine-duct systems, AIAA Journal, 13 (1975) 130-153.

29) X.D. Li, C. Schemel, U. Michel, F. Thiele, Azimuthal sound mode propagation in axisymmetric flow ducts, AIAA Journal, 42 (2004) 2019-2027.

30) W. Eversman, Theoretical model for duct acoustic propagation and radiation, Aeroacoustics of Flight Vehicles: Theory and Practice-Volume 2: Noise Control, NASA RP-1258 (1991) 101-164.

31) R. Ewert, W. Schröder, Acoustic perturbation equations based on flow decomposition via source filtering, Journal of Computational Physics, 188 (2003) 365-398.

32) G. Ashcroft, X. Zhang, Optimized prefactored compact scheme, Journal of Computational Physics, 190 (2003) 459-477.

33) F. Hu, M. Hussaini, J. Manthey, Low-dissipation and low-dispersion Runge–Kutta schemes for computational acoustics, Journal of Computational Physics, 124 (1996) 177-191.

34) D. Stanescu, W. Habashi, 2N-storage Runge–Kutta schemes for acoustics, Journal of Computational Physics, 143 (1998) 674–681.

35) C.A. Kennedy, M.H. Carpenter, Comparison of several numerical methods for simulation of compressible shear layer, NASA Technical paper 3484 (1997).

36) K. Aly, Aerodynamic excitation of the diametral modes of internal axisymmetric cavity, PhD Thesis, McMaster University (2008).

37) L. E. Kinsler, A. R. Frey, A. B. Coppens, J. V. Sanders, Fourth edition. Fundamentals of acoustics. New York: John Wilesy & Sons, Inc. (2000).